
Fractal Patterns May Unravel the Intelligence in Next-Token Prediction

Ibrahim Alabdulmohsin¹ Vinh Q. Tran² Mostafa Deghani¹

Abstract

We study the fractal structure of language, aiming to provide a precise formalism for quantifying properties that may have been previously suspected but not formally shown. We establish that language is: (1) *self-similar*, exhibiting complexities at all levels of granularity, with no particular characteristic context length, and (2) *long-range dependent* (LRD), with a Hurst parameter of approximately $H = 0.70 \pm 0.09$. Based on these findings, we argue that short-term patterns/dependencies in language, such as in paragraphs, mirror the patterns/dependencies over larger scopes, like entire documents. This may shed some light on how next-token prediction can lead to a comprehension of the structure of text at multiple levels of granularity, from words and clauses to broader contexts and intents. We also demonstrate that fractal parameters improve upon perplexity-based bits-per-byte (BPB) in predicting downstream performance. We hope these findings offer a fresh perspective on language and the mechanisms underlying the success of LLMs.

1. Introduction

How does next-token prediction in large language models (LLMs) yield remarkably intelligent behavior? Consider, for instance, the two models: Gemini (Anil et al., 2023a) and GPT4 (OpenAI, 2023). These models have demonstrated extraordinary capabilities beyond just mastering language. Their skills extend to quantitative reasoning, creative content creation, document summarization, and even coding, which has prompted some researchers to ponder if there was more to intelligence than “on-the-fly improvisation” (Bubeck et al., 2023). While understanding the exceptional capabilities of LLMs is complex, particularly given the fuzzy meaning of “intelligent” behavior, a possible insight can be drawn from the study of fractals and self-similarity. We elucidate this connection in this work.

¹Google Deepmind ²Google Research. Correspondence to: Ibrahim Alabdulmohsin <ibomohsin@google.com>.

Self-Similarity. Self-similar processes were introduced by Kolmogorov in 1940 (Kolmogorov, 1940). The notion garnered considerable attention during the late 1960s, thanks to the extensive works of Mandelbrot and his peers (Embrechts & Maejima, 2000). Broadly speaking, an object is called “self-similar” if it is invariant across scales, meaning its statistical or geometric properties stay consistent irrespective of the magnification applied to it (see Figure 1). Nature and geometry furnish us with many such patterns, such as coastlines, snowflakes, the Cantor set and the Koch curve. Despite the distinction, self-similarity is often discussed in the context of “fractals,” another term popularized by Mandelbrot in his seminal book *The Fractal Geometry of Nature* (Mandelbrot, 1982). However, the two concepts are different (Gneiting & Schlather, 2004). See Section 2.

In language, in particular, there have been studies arguing for the presence of a self-similar structure. Nevertheless, due to the computational constraints of the past, it was not feasible to holistically model the joint probability distribution of language. As such, linguists often resorted to rudimentary approximations in their arguments, such as by substituting a word with its frequency or length (Ausloos, 2012), or by focusing on the recurrence of a specific, predetermined word (Najafi & Darooneh, 2015; Altmann et al., 2012). These studies fall short of fully capturing the underlying structure of language due to the simplifying assumptions they make, as discussed in Section 4.

Highlighting the self-similar nature of a process can have profound implications. For instance, conventional Poisson models for Ethernet traffic were shown to fail because traffic was self-similar (Crovella & Bestavros, 1995; Leland et al., 1994; Paxson & Floyd, 1995; Willinger et al., 1997). In such cases, recognizing and quantifying this self-similarity had practical applications, such as in the design of buffers in network devices (Leland & Wilson, 1991). Similarly in language, we argue that self-similarity may offer a fresh perspective on the mechanisms underlying the success of LLMs. Consider the illustrative example shown in Figure 1, where the task is to predict the subsequent measurement in a time series, specifically predicting next tokens in a Wikipedia article (see Section 2 for details). The three plots in Figure 1 (top) represent different manifestations of the same process observed across three distinct time scales. Notably, we observe rich details, e.g. burstiness, in *all* of

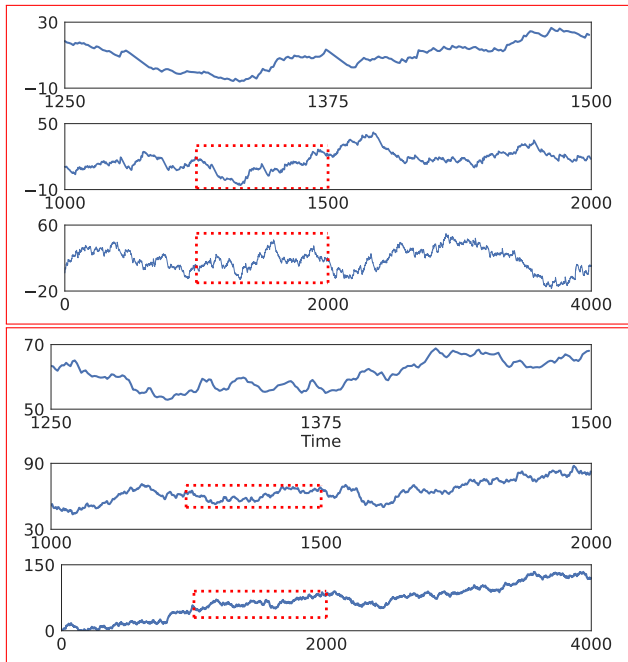


Figure 1. Manifestations of processes across different time scales. A region marked in red corresponds to the magnified plot above it. TOP: The process exhibits self-similarity with rich details at all levels of granularity. It is an integral process $(X_t)_{t \in \mathbb{N}}$ calculated from Wikipedia (see Section 2). BOTTOM: Example of a process that is not self-similar, looking smoother at larger time scales.

them. Hence, for the model to successfully predict the next measurement, it must capture the behavior of the process at various levels of granularity. The standard approach for quantifying self-similarity is the Hölder exponent (Watkins, 2019), which we denote by S . In language, we estimate it to be $S = 0.59 \pm 0.08$, confirming statistical self-similarity.

Why is this significant? We hypothesize that since LLMs are trained to predict the future of a self-similar process, they develop proficiency in capturing behavior across multiple levels of granularity for two interconnected reasons. First, self-similarity implies that the patterns in language at the level of a paragraph are reflective of the patterns seen at the level of a whole text. Hence, recognizing short-term patterns may also aide in learning broader contexts. Second, because language displays detailed, intricate patterns at every level of granularity, it would not be enough to rely only on the immediate context of a sentence to predict the next token. Instead, the model would need to identify patterns at higher levels of granularity; i.e. understand the direction of the argument, and the broader context and intent. It must balance between short- and long-term contexts. Willinger et al. (1995) and Altmann et al. (2012) argue for self-similarity in language precisely because of this hierarchical nature.

Long-range dependence. However, self-similarity by itself

is not sufficient for a predictive model to exhibit anything resembling “intelligent” behavior. In fact, some self-similar processes, despite their intricacy across all levels of granularity, remain entirely unpredictable. A quintessential example is the simple Brownian motion, which is a Wiener process with independent increments. Its discrete analog B_n is defined by $B_n = \sum_{i=1}^n \varepsilon_i$, where $\varepsilon_i \sim \mathcal{N}(0, \sigma^2)$. Despite possessing rich details at all granularities, a model trained to predict B_n cannot obviously acquire any intelligence since the process itself has independent increments.

Thus, for intelligent behavior to manifest, the process must have some degree of predictability or *dependence* as well. One classical metric for quantifying predictability in a stochastic process is the Hurst parameter (Hurst, 1951), developed by the hydrologist H. E. Hurst in 1951 while studying the Nile river flooding. It is generally considered to be a robust metric (Willinger et al., 1995), unlike for instance the wavelet estimator (Abry et al., 1995) and the periodogram method (Geweke & Porter-Hudak, 1983) that can be sensitive to errors (Pilgrim & Taylor, 2018). As discussed in Section 2.3, we estimate the Hurst parameter in language to be $H = 0.70 \pm 0.09$. For context, H can only take values in $[0, 1]$. A higher value suggests more predictability or persistence in the data, while a lower Hurst parameter indicates more randomness ($H = 0.5$ for completely random systems).

While it is compelling that our estimate of H in language lies nearly *midway* between predictability ($H = 1$) and noise ($H = 0.5$), a Hurst parameter of about 0.75 turns out to occur commonly in nature, including in river discharges, Ethernet traffic, temperatures, precipitation, and tree rings (Crovella & Bestavros, 1995; Feller, 1951; Aref, 1998). For agents that learn from data, such as LLMs, this value is also reminiscent of processing-based theories of curiosity, which suggest that a sweet spot of complexity exists (not too simple, nor too unpredictable) that facilitates or accelerates learning (Kidd & Hayden, 2015).

Importantly, predictability and self-similarity *together* imply long-range dependence (LRD). This follows from the definition of self-similarity, where the patterns at small scales mirror those at larger scales so, for example, the correlations established at micro levels are also pertinent at macro levels. LRD is arguably necessary for intelligence to emerge in a predictive model because processes with only short-range dependence could be forecasted (somewhat trivially) with lookup tables that provide the likelihood of transitions over brief sequences. By contrast, this is not possible in LRD processes whose contexts extend indefinitely into the past.

From a practical standpoint, we demonstrate in Section 3 that incorporating fractal parameters can markedly enhance the ability to predict downstream performance in LLMs, compared to perplexity-based metrics alone, such as bits-

per-byte (BPB). Specifically, we introduce a new metric averaging H with $1/\text{BPB}$ and show that using it to predict downstream performance can increase the adjusted R^2 from approximately 0.65 when using solely BPB, to over 0.86 with the new metric. We do not observe improvements when predicting rankings, however.

Statement of Contribution. In summary, we:

1. highlight how the fractal structure of language can offer a unique perspective on the intelligent behavior exhibited by LLMs, and provide a precise formalism to quantify properties, such as long-range dependence.
2. establish that language is self-similar and long-range dependent. We provide concrete estimates in language of the three parameters: the self-similarity (Hölder) exponent, the Hurst parameter, and the fractal dimension. We also estimate the related Joseph exponent.
3. carry out a comparative study across different model architectures and scales, and different domains, such as ArXiv, GitHub, and Wikipedia, among others.
4. connect fractal patterns with learning. Notably, we show that a “median” Hurst exponent (defined in Section 3) improves upon perplexity-based bits-per-byte (BPB) in predicting downstream performance.

2. Fractal Structure of Language

2.1. Preliminaries

Suppose we have a discrete-time, stationary stochastic process $(x_t)_{t \in \mathbb{N}}$, with $\mathbb{E}[x_t] = 0$ and $\mathbb{E}[x_t^2] = 1$. We will refer to $(x_t)_{t \in \mathbb{N}}$ as the *increment process* to distinguish it from the *integral process* $(X_t)_{t \in \mathbb{N}}$ defined by $X_t = \sum_{k=0}^t x_k$. While $(x_t)_{t \in \mathbb{N}}$ and $(X_t)_{t \in \mathbb{N}}$ are merely different representations of the same data, it is useful to keep both representations in mind. For example, self-similarity is typically studied in the context of integral processes whereas long-range dependence (LRD) is defined on increment processes.

In the literature, it is not uncommon to mistakenly equate parameters that are generally different. For example, the Hurst parameter has had many different definitions in the past that were not equivalent, and Mandelbrot himself had cautioned against this (Mandelbrot, 2002). The reason behind this is because different parameters can agree in the idealized fractional Brownian motion setting, leading some researchers to equate them in general (Watkins, 2019). We will keep the self-similarity exponent S and the Hurst parameter H separate in our discussion.

Experimental Setup. In order to establish self-similarity and LRD in language, we convert texts into sequences of

bits using a large language model (LLM). Specifically, we use PaLM2-L (Unicorn) (Anil et al., 2023b) to calculate the probability of the next token w_t conditioned on its entire prefix $w_{[t-1]} = (w_0, w_1, \dots, w_{t-1})$. By the chain rule (Cover, 1999), the corresponding number of bits assigned to w_t is $z_t = -\log p(w_t | w_{[t-1]})$. Unlike in prior works, which rely on simplifications such as by substituting a word with its length (Ausloos, 2012) or by focusing on the recurrence of a single word (Najafi & Darooneh, 2015; Altmann et al., 2012), we use the LLM to approximate the full joint distribution of language. We carry out these calculations for prefixes of up to 2048 tokens (≈ 8 pages of text). Since language is a stochastic process, the sequence of bits of each token conditioned on its past converges asymptotically to the average number of bits required to encode the entire sequence (Cover, 1999). Hence, a suitable normalization, such bits-per-byte (BPB), results in a standardized description of text, consistent across tokenizers. BPB is a widely used as a tokenizer-agnostic metric to compare language modeling performance, e.g. for The Pile (Gao et al., 2020).

Besides PaLM2, we also experiment and report on various model sizes of PaLM (Chowdhery et al., 2022) and decoder-only T5 (Raffel et al., 2019). Namely, we report results for models: PaLM2 XXS (Gecko), XS (Otter), S (Bison), M, and L (Unicorn); PaLM 8B, 62B, 540B; and decoder-only T5.1.1 at Base (110M), Large (341M), XL (1.2B), and XXL (5B) sizes. For PaLM and PaLM2, we use the checkpoints pretrained in Chowdhery et al. (2022) and Anil et al. (2023b). All T5.1.1 decoder baselines, on the other hand, are trained with a casual language modeling objective for 262B tokens of C4 (Raffel et al., 2019). More details on how we train our T5.1.1 baselines can be found in Appendix A.

To rely on LLM for such analysis, it must provide probability scores that are reasonably well-calibrated. Generally, LLMs are known to produce calibrated probability scores at the token level (Kadavath et al., 2022). In Figure 3, we reconfirm this by comparing the logits, $-\log p(\text{word})$, predicted by one of the small language models we use in our study (PaLM-8B) with the actual log probabilities derived from the Google Web Trillion Word Corpus (Brants & Franz, 2006) based on word frequencies. We use histogram binning (by grouping similar logits together) and plot their averaged actual log probabilities, similar to how the expected calibration error (ECE) is calculated (Guo et al., 2017). Notably, we find a strong agreement for the most frequently occurring words, i.e., when the word probability exceeds $p \gg 10^{-9}$.

Once z_t is computed for a document, we construct the increment process $(x_t)_{t \in \mathbb{N}}$ by normalizing z_t to have a zero-mean and unit variance. The integral process $(X_t)_{t \in \mathbb{N}}$ is calculated based on $(x_t)_{t \in \mathbb{N}}$, as described earlier and depicted in Figure 1 (top). Normalizing bits (to have zero mean and unit variance) models language as a random walk. It is a

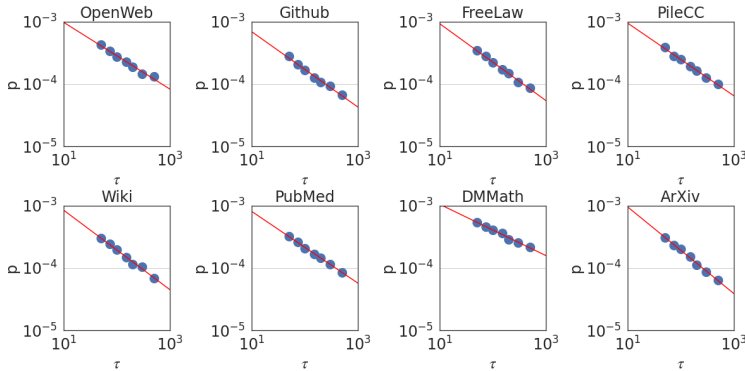


Figure 2. Peak probability $p_\epsilon(\tau)$ is plotted against the granularity level τ (see Section 2.2). We observe a power law $p_\epsilon(\tau) \sim \tau^{-S}$ in all domains, indicating a self-similar structure, with a median self-similarity exponent of $S = 0.59 \pm 0.08$.

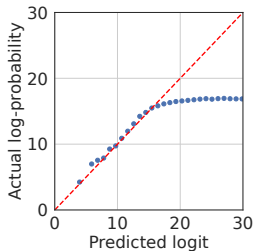


Figure 3. Comparison of PaLM-8B’s logits with actual log-probabilities. We observe a substantial agreement except for exceedingly uncommon words with a probability $< 10^{-9}$. This is consistent with reported findings that LLMs produce calibrated probability scores for tokens; e.g. (Kadavath et al., 2022).

standard approach used extensively in the literature in various contexts, such as in DNA sequences (Peng et al., 1992; Roche et al., 2003; Montemurro & Pury, 2002; Kokol & Podgorelec, 2000; Schenkel et al., 1993).

For analysis, we use The Pile validation split (Gao et al., 2020), consisting of 22 subdomains such as Wikipedia and GitHub. We restrict analysis to sufficiently-long documents of length $> 4K$ tokens and use the first 2K tokens only, to sidestep potential effects of the finite length of documents and the model context. To mitigate noise, only domains with $> 1K$ documents are compared; we report results for them separately and their median. We use bootstrapping (Efron & Tibshirani, 1994) to estimate the error margin.

Notation. We write $f(x) \sim x^c$ if $f(x) = x^c L(x)$ for some slowly-varying function L ; i.e. $L(tx)/L(x) \rightarrow 1$ as $x \rightarrow \infty$ for all $t > 0$. Examples of slowly varying functions are constants $L(x) = c$ and $L(x) = \log x$. When $f(x) \sim x^c$, we will abuse terminology slightly by referring to $f(x)$ as a power law function.

2.2. Self-similarity exponent

An integral process is said to be self-similar if it exhibits *statistical* self-similarity. More precisely, $(X_t)_{t \in \mathbb{N}}$ is self-similar if $(X_{\tau t})_{t \in \mathbb{N}}$ is distributionally equivalent to $(\tau^S X_t)_{t \in \mathbb{N}}$ for some exponent S . Thus, scaling of time is equivalent to an appropriate scaling of space. We will refer to τ as the *granularity level* and to the exponent S as the self-similarity exponent. It is worth noting that S is also called the Hölder exponent (Watkins, 2019). Many time series in nature exhibit self-similar structures, such as human blood pressure and heart rate (Goldberger et al., 2002).

One approach for calculating the self-similarity exponent S is as follows. First, fix $\epsilon \ll 1$ and denote the τ -increments by $(X_{t+\tau} - X_t)_{t \in \mathbb{N}}$. These would correspond, for instance, to the number of bits used for clauses, sentences, paragraphs and longer texts as τ increases. In terms of the increment process $(x_t)_{t \in \mathbb{N}}$, this corresponds to aggregating increments into “bursts”. Let $p_\epsilon(\tau)$ be the probability mass of the event $\{|X_{t+\tau} - X_t| \leq \epsilon\}_{t \in \mathbb{N}}$. Then, S can be estimated by fitting a power law relation $p_\epsilon(\tau) \sim \tau^{-S}$ (Watkins, 2019).

Figure 2 (top) plots the probability $p_\epsilon(\tau)$ against τ when $\epsilon = 5 \times 10^{-3}$ using PaLM2-L. We indeed observe a power law relation; i.e. linear in a log-log scale, with a median self-similarity exponent of $S = 0.59 \pm 0.08$. Section 3 shows that the median S is robust to the choice of the LLM.

2.3. Hurst parameter

The Hurst parameter $H \in [0, 1]$ quantifies the degree of predictability or dependence over time (Hurst, 1951). It is calculated using the so-called rescaled-range (R/S) analysis. Let $(x_t)_{t \in \mathbb{N}}$ be an increment process. For each $n \in \mathbb{N}$, write $y_t = x_t - \frac{1}{t} \sum_{k=0}^t x_k$ and $Y_t = \sum_{k=0}^t y_t$. The range and scale are defined, respectively, as $R(n) = \max_{t \leq n} Y_t - \min_{t \leq n} Y_t$ and $S(n) = \sigma(\{x_k\}_{k \leq n})$, where σ is the standard deviation. Then, the Hurst parameter H is

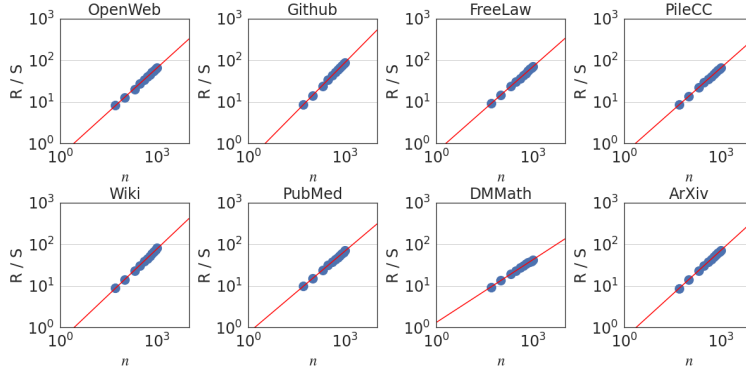


Figure 4. Rescaled range $R(n)/S(n)$ is plotted against the number of normalized bits n . We observe a power law $R(n)/S(n) \sim n^H$ in all domains. When aggregating all datasets, $H = 0.70 \pm .01$, indicating long-range dependence (LRD).

estimated by fitting a power law relation $R(n)/S(n) \sim n^H$. As stated earlier, for completely random processes, such as a simple Brownian motion, it can be shown that $H = 1/2$. In addition, $H > 1/2$ implies dependence over time (Crovella & Bestavros, 1995; Willinger et al., 1995; Aref, 1998).

Writing $\rho_n = \mathbb{E}[(x_{t+n}x_t)]$ for the autocovariance function of the increment process $(x_t)_{t \in \mathbb{N}}$, the Hurst parameter satisfies $H = 1 - \beta/2$ when $\rho_n \sim n^{-\beta}$ as $n \rightarrow \infty$ (Gneiting & Schlather, 2004; Crovella & Bestavros, 1995). Since in self-similar processes, $H > 1/2$ implies long-range dependence (LRD), LRD is equivalent to the condition that the autocovariances are not summable. In terms of the integral process, it can be shown that (Samorodnitsky, 2006):

$$\lim_{n \rightarrow \infty} \frac{\text{Var}(X_n)}{n} = 1 + 2 \sum_{i=1}^{\infty} \rho_i. \quad (1)$$

Hence, if $H < 1/2$, the auto-covariances are summable and $\text{Var}(X_n)$ grows, at most, linearly fast on n . On the other hand, if the process has LRD, $\text{Var}(X_n)$ grows superlinearly on n . In particular, using the Euler-Maclaurin summation formula (Apostol, 1999; Alabdulmohsin, 2018), one obtains $\text{Var}(X_n) \sim n^{2H}$ if $H > 1/2$. Figure 4 plots the rescaled range $R(n)/S(n)$ against n . We observe a power law relation with a median Hurst parameter of $H = 0.70 \pm 0.09$.

2.4. Fractal dimension

Broadly speaking, the fractal dimension of an object describes its *local* complexity. For a geometric object Z , such as the Koch curve, let τ be a chosen scale (e.g. a short ruler for measuring lengths or a small square for areas). Let $N(\tau)$ be the minimum number of objects of scale τ that cover Z . Then, the fractal dimension of Z , also called its Hausdorff dimension, is: $D = -\lim_{\tau \rightarrow 0} \left\{ \frac{\log N(\tau)}{\log \tau} \right\}$ (Pilgrim & Taylor, 2018). For example, a line has a fractal dimension 1, in agreement with its topological dimension, because $N(\tau) = C/\tau$ for some constant $C > 0$.

By convention, an object is referred to as ‘‘fractal’’ if D is different from its topological dimension. For example, the fractal dimension of the Koch curve is about 1.26 when its topological dimension is 1. Fractals explain some puzzling observations, such as why estimates of the length of the coast of Britain varied significantly from one study to another, because lengths in fractals are scale-sensitive. Mandelbrot estimated the fractal dimension of the coast of Britain to be 1.25 (Mandelbrot, 1967).

The definition above for the fractal dimension D applies to geometric shapes, but an analogous definition has been introduced for stochastic processes. Let $(x_t)_{t \in \mathbb{R}}$ be a stationary process with autocovariance ρ_n . Then, its fractal dimension D is determined according to the local behavior of ρ_n at the vicinity of $n = 0$, by first normalizing $(x_t)_{t \in \mathbb{R}}$ to have a zero-mean and a unit variance, and modeling ρ_n using a power law $\rho_n \sim 1 - n^\alpha$ as $n \rightarrow 0^+$, for $\alpha \in (0, 2]$. Then, the fractal dimension $D \in [1, 2]$ of $(x_t)_{t \in \mathbb{R}}$ is defined by $D = 2 - \alpha/2$ (Gneiting & Schlather, 2004). A value $D \gg 1$ indicates a significant fractal structure.

It can be shown that $D = 2 - S$, where S is the self-similarity exponent (Gneiting & Schlather, 2004). For language, this gives a median fractal dimension of $D = 1.41 \pm 0.08$.

2.5. Joseph effect

Next, we examine another related parameter that is commonly studied in self-similar processes. The motivation behind it comes from the fact that in processes with LRD, one often observes *burstiness* as shown in Figure 1; i.e. clusters over time in which the process fully resides on one side of the mean, before switching to the other. This is quite unlike random noise, for instance, where measurements are evenly distributed on both sides of the mean. The effect is often referred to as the Joseph effect, named after the biblical story of the seven fat years and seven lean years (Willinger et al., 1995; Mandelbrot & Wallis, 1968; Watkins, 2019).

Fractal Patterns May Unravel the Intelligence in Next-Token Prediction

	OpenWeb	GitHub	FreeLaw	PileCC	Wiki	PubMed	Math	ArXiv
S	0.53 ± .05	0.60 ± .05	0.61 ± .05	0.56 ± .03	0.62 ± .02	0.60 ± .07	0.42 ± .03	0.70 ± .03
H	0.68 ± .01	0.79 ± .01	0.68 ± .00	0.70 ± .00	0.74 ± .01	0.65 ± .00	0.50 ± .01	0.72 ± .01
J	0.46 ± .01	0.49 ± .00	0.49 ± .00	0.50 ± .00	0.52 ± .00	0.44 ± .00	0.28 ± .00	0.49 ± .00

Table 1. A comparison of the fractal parameters across 8 different domains with > 1000 documents each in The Pile benchmark (see Section 2.1 for selection criteria). DM-Mathematics is markedly different because each document consists of questions, with no LRD.

	T5-Decoder				PaLM			PaLM2				
	110M	340M	1B	5B	8B	62B	540B	XXS	XS	S	M	L
S	.58±.06	.60±.06	.60±.05	.58±.08	.60±.07	.62±.08	.64±.08	.59±.06	.57±.08	.56±.05	.59±.07	.60±.08
H	.64±.08	.64±.08	.64±.09	.64±.08	.66±.07	.68±.07	.68±.07	.66±.07	.66±.07	.67±.08	.68±.09	.69±.09
J	.44±.06	.44±.06	.44±.06	.44±.06	.47±.06	.47±.06	.48±.06	.47±.06	.47±.06	.48±.07	.48±.07	.49±.08

Table 2. A comparison of the estimated median fractal parameters by various LLMs over the entire Pile validation split. Estimates are generally robust to the choice of the LLM, but the tiny variations in median H reflect improvements in the model quality. See Section 3.

A common way to quantify the Joseph effect for integral processes $(X_t)_{t \in \mathbb{N}}$ is as follows (Watkins, 2019). First, let σ_τ be the standard deviation of the τ -increments $X_{t+\tau} - X_t$. Then, fit a power law relation $\sigma_\tau \sim \tau^J$. The exponent J here is called the Joseph exponent. In an idealized fractional Brownian motion, both J and the self-similarity exponent S coincide. Figure 5 provides the detailed empirical results. Overall, we obtain an estimate of $J = 0.49 \pm 0.08$, which is intriguing because $J = 0.5$ corresponds to self-similar processes with independent increments.

3. Analysis

Comparative Analysis. Table 1 compares the estimated fractal parameters across different domains, such as ArXiv, Github and Wikipedia. In general, most domains share similar self-similarity and Hurst exponents with a few exceptions. The first notable exception is DM-Mathematics, which has a Hurst parameter of about 0.5. To recall, a value of $H = 0.5$ indicates that the data does not exhibit long-range dependence (LRD). Upon closer inspection, however, a value of $H = 0.5$ is not surprising for DM-Mathematics because its documents consist of independent mathematical questions as shown in Figure 7. The second notable observation is the relatively larger value of $H = 0.79$ in GitHub, indicating more structure in code. This is in agreement with earlier findings by Kokol & Podgorelec (2000) who estimated LRD in computer languages to be greater than in nature language. In Table 2, we compare the three fractal parameters S, H and J using different families of LLM and different model sizes. Overall, we observe that the estimated parameters are generally robust to the choice of the architecture.

Downstream Performance. By definition, fractal parameters are calculated on the sequence of log-perplexity scores after normalizing them to zero-mean and unit variance. Hence, they may offer an assessment of downstream perfor-

mance that improves upon using a perplexity-based metric like bits-per-byte (BPB) alone.

To test this hypothesis, we evaluate the 12 models in Table 2 on challenging downstream zero- and few-shot benchmarks focusing on language understanding and reasoning. We include results for 0-shot (0S) and 3-shot (3S) evaluation for BIG-Bench Hard tasks (Srivastava et al., 2022; Suzgun et al., 2022) reporting both direct and chain-of-thought (CoT) prompting results following Chung et al. (2022). In addition we report 0-shot and 5-shot (5S) MMLU (Hendrycks et al., 2020), and 8-shot (8S) GSM8K (Cobbe et al., 2021) with CoT. Raw accuracy is reported for all tasks. BBH and MMLU scores are averaged across all 21 tasks and 57 subjects, respectively. All prompt templates for our evaluation are taken from Chung et al. (2022); Longpre et al. (2023), which we refer the reader to for more details. We prompt all models using a 2048 context length. See Table 9 of Appendix C for the full results.

The first (surprising) observation is that the median Hurst parameter is itself strongly correlated with the BPB scores with an absolute Pearson correlation coefficient of 0.83, even though the Hurst exponent is calculated after normalizing all token losses to zero-mean and unit variance! Informally, this implies that second-order statistics on the sequence of token losses of a particular model can predict its mean! The self-similarity exponent, by contrast, has an absolute Pearson correlation of 0.23 with BPB.

Figure 6 displays downstream performance against both the median Hurst exponent and the median BPB score, where median values are calculated on the 8 domains in The Pile benchmark listed in Table 1. In general, both the BPB score and the median Hurst are good predictors of downstream performance. However, we observe that improvements in BPB alone without impacting the median Hurst exponent do not directly translate into improvements downstream.

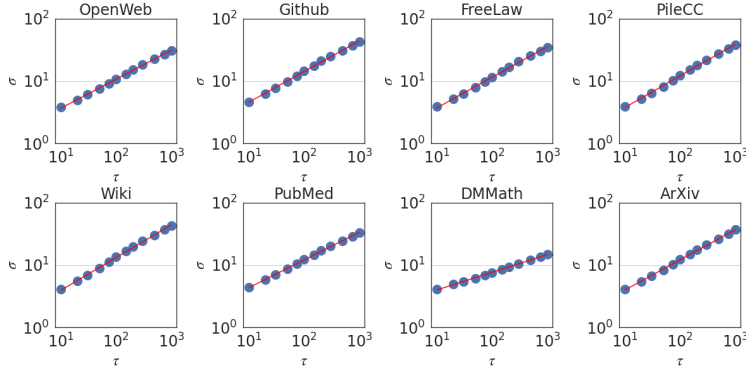


Figure 5. The standard deviation σ of the τ -increments $X_{t+\tau} - X_t$ is plotted against the scale τ . We, again, observe another power law relation $\sigma \sim \tau^J$, with a Joseph exponent $J = 0.49 \pm 0.08$.

	Magnitude			Ranking	
	BPB	H	H_B	BPB	H_B
0S BBH Direct	0.785	0.841	0.883	0.958	0.958
0S MMLU	0.653	0.831	0.825	0.769	0.769
0S BBH+MMLU	0.685	0.849	0.852	0.930	0.930
3S BBH Direct	0.767	0.895	0.926	1.000	1.000
3S BBH CoT	0.881	0.892	0.979	1.000	1.000
5S MMLU	0.660	0.853	0.832	0.783	0.783
8S GSM8K CoT	0.654	0.867	0.851	0.993	0.993
FS BBH+MMLU+GSM8K	0.717	0.890	0.891	1.000	1.000

Table 3. Adjusted R^2 , which measures the proportion of variation in downstream performance (row) predictable by a linear regressor with the given input (column). The combined metric $H_B = 1/\text{BPB} + H$ predicts downstream performance better in all downstream metrics, compared to BPB alone. S and J do not yield such improvements (see Appendix C). For ranking, we report Spearman correlations, which suggest that BPB is sufficient.

This is verified quantitatively in Table 3, which reports the adjusted R^2 values – the proportion of variance in each downstream metric that can be predicted using BPB, H, or by combining them together into $H_B = 1/\text{BPB} + H$, with BPB replaced with its reciprocal so that higher values are better. We observe that H_B yields indeed a stronger predictor of downstream performance. For ranking, however, BPB alone is sufficient. See Appendix C for similar analysis using the exponents S and J.

Context Length at Training Time. Finally, self-similarity and long-range dependence point to an intriguing possibility: the importance of *training* the model with extensive contexts in order to capture the fractal-nature of language, which may elevate the model’s capabilities regardless of the context length needed during inference. To test this hypothesis, we pretrain three decoder-only T5.1.1 models with 1B parameters on SlimPajama-627B (Sobolva et al., 2023) for up to 100B tokens using three context

	2K	4K	8K
0S BBH Direct	1.81	1.68	1.76
0S MMLU	25.73	26.04	25.81
0S BBH+MMLU	13.39	13.49	13.42
3S BBH Direct	21.35	24.76	23.14
3S BBH CoT	16.87	12.21	7.14
5S MMLU	26.57	26.69	27.07
8S GSM8K CoT	1.06	1.21	1.74
FS BBH + MMLU+GSM8K	15.58	15.46	14.65

Table 4. Downstream performance comparison for three decoder-only T5.1.1. models pretrained on 100B tokens with either 2K, 4K, or 8K context lengths.

lengths: 2K, 4K and 8K, all observing the same number of tokens per batch. We use SlimPajama-627B instead of C4 because most documents in C4 are short ($\approx 94\%$ of them are $< 2K$ tokens in length). Refer to Appendix A for details. These models are, then, evaluated on the same downstream benchmarks listed in Figure 6 and Table 3. As shown in Table 4, however, we do not observe any improvements in performance with context length in this particular setup.

4. Related Works

The statistical attributes of human language have long piqued scholarly curiosity, such as One example is Zipf’s law, which Shannon leveraged to estimate the entropy of English to be around 1 bit per letter (Shannon, 1951), but his calculation did not consider second-order statistics. More recently, Eftekhari (2006) proposed a refinement to Zipf’s law, suggesting its application to letters rather than words. Another related result is Heap’s law, which states that the number of unique words in a document is a power law function of the document’s length (Heaps, 1978). However, both Zipf’s and Heap’s laws are invariant to the semantic ordering of text, so they do not capture important aspects, such as long-range dependence (LRD) (Najafi & Darooneh, 2015).

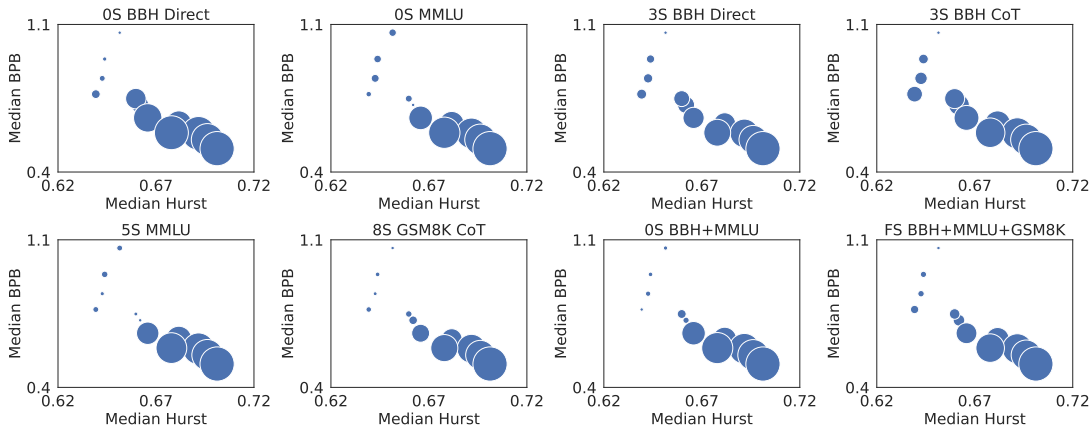


Figure 6. Downstream metric, indicated by bubble size, is plotted vs. the median Hurst and the median BPB for all 12 language models.

Document I: What is the square root of 211269 to the nearest integer? 460. What is the square root of 645374 to the nearest integer? 803...

Document II: Suppose $5 \cdot 1 = r - 35$, $-2 \cdot r + 5 \cdot 1 - 15 = -70$. Is r a multiple of 4? True. Suppose $2 \cdot 1 + 11 - 1 = 0$. Does 15 divide $(-2)/1 - 118/(-5)$? False...

Figure 7. Two examples of documents from the DM-Mathematics subset of The Pile benchmark (Gao et al., 2020). Each document comprises of multiple independent questions. The lack of LRD in this data is reflected in its Hurst parameter of $H = 0.50 \pm 0.01$

In terms of self-similarity in language, the Menzerath-Altmann law stipulates a self-similar behavior in the following sense: when the size of a language construct increases, the size of its constituents decreases, and this happens at all scales (Najafi & Darooneh, 2015; Andres, 2009). In Ausloos (2012), the authors model texts as a time series by replacing a word with its length. After that, they study the fractal behavior of language. However, replacing a word with its length is invalid because it is not translation-independent (i.e. one could map every word to an arbitrary token, including tokens of equal length). In our work, we model language as a time series of bits calculated from conditional entropies, reflecting the structure of the language itself.

In Najafi & Darooneh (2015), the authors define a fractal dimension for each word. Informally, they examine the recurrence of a single, predetermined word in texts as an ON/OFF time series, similar to the approach used in Altmann et al. (2012). However, this is only applicable to individual words and cannot model higher-level clauses. For instance, it does not distinguish between the word “time” in the phrase “once upon a time” and the word “time” in “space and time.” Kokol & Podgorelec (2000) estimate LRD

in natural language, and suggest that its LRD is close to that of pure noise! They conjecture this was due to the use of ASCII encoding. In computer languages, they observe LRD and suggest this is because computer languages are formal.

Besides the above concerns in prior studies that examined the self-similar structure in language, another concern is that they sometimes give extremely large values of the fractal dimension, sometimes even exceeding 10 (Andres, 2009). Such values are difficult to interpret because classical definitions of the fractal dimension restrict its value to the range $[1, 2]$ for time series. We do not observe such issues in our analysis. In our case, $D = 1.41 \pm 0.08$.

5. Concluding Remarks

In this work, we highlight intriguing insights into the underlying fractal structure of language and how it may be interconnected with the intelligent behavior of LLMs. Our formalism quantifies properties of language that may have been suspected, but not previously formally shown. In particular, the need in LLMs to balance between short- and long-term contexts is reflected in the self-similar structure of language, while long-range dependence is quantifiable using the Hurst parameter. For instance, the absence of LRD in DM-Mathematics is reflected in its Hurst parameter of $H \approx 0.5$. Interestingly, the estimated median Hurst value of $H = 0.70 \pm 0.09$ in language reflects an intriguing balance between predictability and noise that is similar to many other phenomena, and combining both H with BPB together yields a stronger predictor of downstream performance. We carry out an extensive comparative analysis across different domains and model architectures, revealing that fractal parameters are generally robust. We hope that future research can further probe into these fractal properties, unearthing deeper understandings of the relation between intelligence and language.

6. Acknowledgement

The authors would like to thank Justin Gilmer and Olivier Bousquet for their feedback on earlier drafts of this manuscript, and both Google Deepmind and Google Research teams at large for the insightful discussions and providing a supportive research environment.

7. Potential Broader Impact

This paper presents work whose goal is to advance the field of Machine Learning. There are many potential societal consequences of our work, none which we feel must be specifically highlighted here.

References

- Abry, P., Gonçalves, P., and Flandrin, P. Wavelets, spectrum analysis and 1/f processes. *Wavelets and statistics*, pp. 15–29, 1995.
- Alabdulmohsin, I. M. *Summability calculus: A comprehensive theory of fractional finite sums*. Springer, 2018.
- Altmann, E. G., Cristadoro, G., and Esposti, M. D. On the origin of long-range correlations in texts. *Proceedings of the National Academy of Sciences*, 109(29):11582–11587, 2012.
- Andres, J. On de Saussure’s principle of linearity and visualization of language structures. *Glottology*, 2(2):1–14, 2009.
- Anil, R., Borgeaud, S., Wu, Y., Alayrac, J.-B., Yu, J., Soricut, R., Schalkwyk, J., Dai, A. M., Hauth, A., Millican, K., Silver, D., Petrov, S., Johnson, M., Antonoglou, I., Schrittwieser, J., Glaese, A., Chen, J., Pitler, E., et al. Gemini: A family of highly capable multimodal models. *arXiv:2312.11805v1 [cs.CL]*, 2023a.
- Anil, R., Dai, A. M., Firat, O., Johnson, M., Lepikhin, D., Passos, A., Shakeri, S., Taropa, E., Bailey, P., Chen, Z., Chu, E., Clark, J. H., Shafey, L. E., Huang, Y., Meier-Hellstern, K., Mishra, G., Moreira, E., Omernick, M., Robinson, K., Ruder, S., Tay, Y., Xiao, K., Xu, Y., Zhang, Y., Abrego, G. H., Ahn, J., Austin, J., Barham, P., Botha, J., Bradbury, J., Brahma, S., Brooks, K., Catasta, M., Cheng, Y., Cherry, C., Choquette-Choo, C. A., Chowdhery, A., Crepy, C., Dave, S., Dehghani, M., Dev, S., Devlin, J., Díaz, M., Du, N., Dyer, E., Feinberg, V., Feng, F., Fienber, V., Freitag, M., Garcia, X., Gehrmann, S., Gonzalez, L., Gur-Ari, G., Hand, S., Hashemi, H., Hou, L., Howland, J., Hu, A., Hui, J., Hurwitz, J., Isard, M., Ittycheriah, A., Jagielski, M., Jia, W., Kenealy, K., Krikun, M., Kudugunta, S., Lan, C., Lee, K., Lee, B., Li, E., Li, M., Li, W., Li, Y., Li, J., Lim, H., Lin, H., Liu, Z., Liu, F., Maggioni, M., Mahendru, A., Maynez, J., Misra, V., Moussalem, M., Nado, Z., Nham, J., Ni, E., Nystrom, A., Parrish, A., Pellat, M., Polacek, M., Polozov, A., Pope, R., Qiao, S., Reif, E., Richter, B., Riley, P., Ros, A. C., Roy, A., Saeta, B., Samuel, R., Shelby, R., Slone, A., Smilkov, D., So, D. R., Sohn, D., Tokumine, S., Valter, D., Vasudevan, V., Vodrahalli, K., Wang, X., Wang, P., Wang, Z., Wang, T., Wieting, J., Wu, Y., Xu, K., Xu, Y., Xue, L., Yin, P., Yu, J., Zhang, Q., Zheng, S., Zheng, C., Zhou, W., Zhou, D., Petrov, S., and Wu, Y. PaLM 2 technical report. *arXiv:2305.10403v3 [cs.CL]*, 2023b.
- Apostol, T. M. An elementary view of Euler’s summation formula. *The American Mathematical Monthly*, 106(5): 409–418, 1999.
- Aref, S. Hurst phenomenon and fractal dimensions in long-term yield data. In *Conference on Applied Statistics in Agriculture*, 1998.
- Ausloos, M. Generalized Hurst exponent and multifractal function of original and translated texts mapped into frequency and length time series. *Physical Review E*, 86(3): 031108, 2012.
- Bradbury, J., Frostig, R., Hawkins, P., Johnson, M. J., Leary, C., Maclaurin, D., Necula, G., Paszke, A., VanderPlas, J., Wanderman-Milne, S., and Zhang, Q. JAX: composable transformations of Python+NumPy programs, 2018. URL <http://github.com/google/jax>.
- Brants, T. and Franz, A. Web 1T 5-gram Version 1, 2006. URL <https://catalog.ldc.upenn.edu/LDC2006T13>. Web Download. Philadelphia: Linguistic Data Consortium.
- Bubeck, S., Chandrasekaran, V., Eldan, R., Gehrke, J., Horvitz, E., Kamar, E., Lee, P., Lee, Y. T., Li, Y., Lundberg, S., Nori, H., Palangi, H., Ribeiro, M. T., and Zhang, Y. Sparks of artificial general intelligence: Early experiments with GPT-4, 2023.
- Chowdhery, A., Narang, S., Devlin, J., Bosma, M., Mishra, G., Roberts, A., Barham, P., Chung, H. W., Sutton, C., Gehrmann, S., et al. PaLM: Scaling language modeling with pathways. *arXiv preprint arXiv:2204.02311*, 2022.
- Chung, H. W., Hou, Le and, L. S., Zoph, B., Tay, Y., Fedus, W., and et al. Scaling instruction-finetuned language models. *arXiv:2210.11416v5 [cs.LG]*, 2022.
- Cobbe, K., Kosaraju, V., Bavarian, M., Hilton, J., Nakano, R., Hesse, C., and Schulman, J. Training verifiers to solve math word problems. *arXiv:2110.14168v2 [cs.LG]*, 2021.
- Cover, T. M. *Elements of information theory*. John Wiley & Sons, 1999.

- Crovella, M. E. and Bestavros, A. Explaining world wide web traffic self-similarity. Technical report, Boston University Computer Science Department, 1995.
- Efron, B. and Tibshirani, R. J. *An introduction to the bootstrap*. CRC press, 1994.
- Eftekhari, A. Fractal geometry of texts: An initial application to the works of Shakespeare. *Journal of Quantitative Linguistics*, 13(2-3):177–193, 2006. doi: 10.1080/09296170600850106.
- Embrechts, P. and Maejima, M. An introduction to the theory of self-similar stochastic processes. *International journal of modern physics B*, 14(12n13):1399–1420, 2000.
- Feller, W. The Asymptotic Distribution of the Range of Sums of Independent Random Variables. *The Annals of Mathematical Statistics*, 22(3):427 – 432, 1951. doi: 10.1214/aoms/1177729589. URL <https://doi.org/10.1214/aoms/1177729589>.
- Gao, L., Biderman, S., Black, S., Golding, L., Hoppe, T., Foster, C., Phang, J., He, H., Thite, A., Nabeshima, N., Presser, S., and Leahy, C. The Pile: An 800GB dataset of diverse text for language modeling. *arXiv:2101.00027v1 [cs.CL]*, 2020.
- Geweke, J. and Porter-Hudak, S. The estimation and application of long memory time series models. *Journal of time series analysis*, 4(4):221–238, 1983.
- Gneiting, T. and Schlather, M. Stochastic models that separate fractal dimension and the Hurst effect. *SIAM Review*, 46(2):269–282, 2004. doi: 10.1137/s0036144501394387.
- Goldberger, A. L., Amaral, L. A., Hausdorff, J. M., Ivanov, P. C., Peng, C.-K., and Stanley, H. E. Fractal dynamics in physiology: alterations with disease and aging. *Proceedings of the national academy of sciences*, 99(suppl.1): 2466–2472, 2002.
- Guo, C., Pleiss, G., Sun, Y., and Weinberger, K. Q. On calibration of modern neural networks. In *ICML*. PMLR, 2017.
- Heaps, H. S. *Information retrieval, computational and theoretical aspects*. Academic Press, 1978.
- Hendrycks, D., Burns, C., Basart, S., Zou, A., Mazeika, M., Song, D., and Steinhardt, J. Measuring massive multitask language understanding. *arXiv preprint arXiv:2009.03300*, 2020.
- Hurst, H. E. Long-term storage capacity of reservoirs. *Transactions of the American society of civil engineers*, 116(1): 770–799, 1951.
- Jouppi, N. P., Yoon, D. H., Kurian, G., Li, S., Patil, N., Laudon, J., Young, C., and Patterson, D. A domain-specific supercomputer for training deep neural networks. *Communications of the ACM*, 63(7):67–78, 2020.
- Kadavath, S., Conerly, T., Askell, A., Henighan, T., Drain, D., Perez, E., Schiefer, N., Hatfield-Dodds, Z., DasSarma, N., Tran-Johnson, E., et al. Language models (mostly) know what they know. *arXiv preprint arXiv:2207.05221*, 2022.
- Kidd, C. and Hayden, B. Y. The psychology and neuroscience of curiosity. *Neuron*, 88(3):449–460, 2015.
- Kokol, P. and Podgorelec, V. Complexity and human writings. *Complexity*, 7:1–6, 2000.
- Kolmogorov, A. N. Wiener’sche spiralen und einige andere interessante kurven in hilbertscen raum, cr (doklady). *Acad. Sci. URSS (NS)*, 26:115–118, 1940.
- Leland, W. E. and Wilson, D. V. High time-resolution measurement and analysis of LAN traffic: Implications for LAN interconnection. In *IEEE INFCOM*, 1991.
- Leland, W. E., Taqqu, M. S., Willinger, W., and Wilson, D. V. On the self-similar nature of Ethernet traffic. *IEEE/ACM Transactions on networking*, 2(1):1–15, 1994.
- Longpre, S., Hou, L., Vu, T., Webson, A., Chung, H. W., Tay, Y., Zhou, D., Le, Q. V., Zoph, B., Wei, J., and Roberts, A. The flan collection: designing data and methods for effective instruction tuning. In *Proceedings of the 40th International Conference on Machine Learning, ICML’23*. JMLR.org, 2023.
- Mandelbrot, B. How long is the coast of Britain? Statistical self-similarity and fractional dimension. *science*, 156 (3775):636–638, 1967.
- Mandelbrot, B. *Gaussian self-affinity and fractals: globality, the earth, 1/f noise, and R/S*. Springer Science and Business Media, 2002.
- Mandelbrot, B. B. *The fractal geometry of nature*. WH freeman New York, 1982.
- Mandelbrot, B. B. and Wallis, J. R. Noah, Joseph, and operational hydrology. *Water resources research*, 4(5): 909–918, 1968.
- Montemurro, M. A. and Pury, P. A. Long-range fractal correlations in literary corpora. *Fractals*, 10(04):451–461, 2002.
- Najafi, E. and Darooneh, A. H. The fractal patterns of words in a text: a method for automatic keyword extraction. *PloS one*, 10(6):e0130617, 2015.

- OpenAI. GPT-4 technical report. *arXiv:2303.08774v4 [cs.CL]*, 2023.
- Paxson, V. and Floyd, S. Wide area traffic: the failure of Poisson modeling. *IEEE/ACM Transactions on networking*, 3(3):226–244, 1995.
- Peng, C.-K., Buldyrev, S. V., Goldberger, A. L., Havlin, S., Sciortino, F., Simons, M., and Stanley, H. E. Long-range correlations in nucleotide sequences. *Nature*, 356(6365): 168–170, 1992.
- Pilgrim, I. and Taylor, R. P. Fractal analysis of time-series data sets: Methods and challenges. In Ouadfeul, S.-A. (ed.), *Fractal Analysis*, chapter 2. IntechOpen, Rijeka, 2018. doi: 10.5772/intechopen.81958. URL <https://doi.org/10.5772/intechopen.81958>.
- Raffel, C., Shazeer, N., Roberts, A., Lee, K., Narang, S., Matena, M., Zhou, Y., Li, W., and Liu, P. J. Exploring the limits of transfer learning with a unified text-to-text transformer. *arXiv:1910.10683v4 [cs.LG]*, 2019.
- Roberts, A., Chung, H. W., Levskaya, A., Mishra, G., Bradbury, J., Andor, D., Narang, S., Lester, B., Gaffney, C., Mohiuddin, A., Hawthorne, C., Lewkowycz, A., Salcianu, A., van Zee, M., Austin, J., Goodman, S., Soares, L. B., Hu, H., Tsvyashchenko, S., Chowdhery, A., Bastings, J., Bulian, J., Garcia, X., Ni, J., Chen, A., Kenealy, K., Clark, J. H., Lee, S., Garrette, D., Lee-Thorp, J., Raffel, C., Shazeer, N., Ritter, M., Bosma, M., Passos, A., Maitin-Shepard, J., Fiedel, N., Omernick, M., Saeta, B., Sepassi, R., Spiridonov, A., Newlan, J., and Gesmundo, A. Scaling up models and data with `t5x` and `seqio`, 2022. URL <https://arxiv.org/abs/2203.17189>.
- Roche, S., Bicout, D., Maciá, E., and Kats, E. Long range correlations in DNA: scaling properties and charge transfer efficiency. *Physical review letters*, 91(22):228101, 2003.
- Samorodnitsky, G. Long memory and self-similar processes. In *Annales de la Faculté des sciences de Toulouse: Mathématiques*, volume 15, pp. 107–123, 2006.
- Schenkel, A., Zhang, J., and Zhang, Y.-C. Long range correlation in human writings. *Fractals*, 1(01):47–57, 1993.
- Shannon, C. E. Prediction and entropy of printed English. *Bell system technical journal*, 30(1):50–64, 1951.
- Shazeer, N. and Stern, M. Adafactor: Adaptive learning rates with sublinear memory cost. In *International Conference on Machine Learning*, pp. 4596–4604. PMLR, 2018.
- Soboleva, D., Al-Khateeb, F., Myers, R., Steeves, J. R., Hestness, J., and Dey, N. SlimPajama: A 627B token cleaned and deduplicated version of RedPajama, June 2023. URL <https://huggingface.co/datasets/cerebras/SlimPajama-627B>.
- Srivastava, A., Rastogi, A., Rao, A., Shoeb, A. A. M., Abid, A., Fisch, A., Brown, A. R., Santoro, A., Gupta, A., Garriga-Alonso, A., et al. Beyond the imitation game: Quantifying and extrapolating the capabilities of language models. *arXiv preprint arXiv:2206.04615*, 2022.
- Suzgun, M., Scales, N., Scharli, N., Gehrmann, S., Tay, Y., Chung, H. W., Chowdhery, A., Le, Q. V., Chi, E. H., Zhou, D., and Wei, J. Challenging BIG-Bench tasks and whether chain-of-thought can solve them. *arXiv:2210.09261v1 [cs.CL]*, 2022.
- Watkins, N. Mandelbrot’s stochastic time series models. *Earth and Space Science*, 6(11):2044–2056, 2019.
- Willinger, W., Taqqu, M. S., Leland, W. E., and Wilson, D. V. Self-similarity in high-speed packet traffic: analysis and modeling of Ethernet traffic measurements. *Statistical science*, pp. 67–85, 1995.
- Willinger, W., Taqqu, M. S., Sherman, R., and Wilson, D. V. Self-similarity through high-variability: statistical analysis of Ethernet LAN traffic at the source level. *IEEE/ACM Transactions on networking*, 5(1):71–86, 1997.

A. Experiment Details

All of our experiments are conducted in JAX/Flax (Bradbury et al., 2018) using the open source T5X framework (Roberts et al., 2022).

T5 baselines in Table 2 and 3 are pretrained from scratch using the open source T5.1.1 decoder-only architecture from the T5X library.¹ We pretrain using a causal language modeling objective over the C4 corpus with the default T5 vocabulary as per Raffel et al. (2019). Training is done for 500k steps with a sequence length of 1024 and batch size of 512, resulting in a total of 262B tokens seen during pretraining. We optimize our model with the Adafactor (Shazeer & Stern, 2018) optimizer with an inverse square root learning rate schedule, 1k warmup steps, and an initial learning rate of 1e-2. Models are trained using 256 TPUv5e chips (Jouppi et al., 2020).

T5 context length ablation experiments in Table 4 are trained with the same pretraining objective but over the SlimPajama-627B corpus (Soboleva et al., 2023) and using a modified version of the T5 vocabulary that preserves whitespace and introduces byte-fallback for out of vocabulary tokens. This is similar to Chowdhery et al. (2022), but preserving the original T5 vocabulary. Models with sequence lengths 2048, 4096, 8192 are trained with batch sizes of 512, 256, and 128 respectively to preserve the number of tokens seen per batch and overall training steps. We train all models for 100k steps, using the same learning rate schedule described above. Hence, all models observe 100B tokens.

¹https://github.com/google-research/t5x/tree/main/t5x/examples/decoder_only/models

B. Full Results

In this section, we provide the full list of parameters calculated for each combination of LLM and domain. We use bootstrapping (Efron & Tibshirani, 1994) to estimate the error margin.

Model	OpenWebText2	Github	FreeLaw	Pile-CC	Wikipedia	PubMed	Mathematics	ArXiv
T5-Decoder-110M	2.89	1.82	2.45	2.88	2.80	2.36	2.28	2.70
T5-Decoder-340M	2.60	1.56	2.14	2.62	2.52	2.08	2.10	2.42
T5-Decoder-1B	2.38	1.37	1.91	2.41	2.29	1.88	2.00	2.19
T5-Decoder-5B	2.19	1.22	1.73	2.25	2.11	1.73	1.91	2.01
PaLM1-8B	2.26	0.79	1.66	2.36	2.08	1.89	1.40	2.08
PaLM1-62B	2.02	0.62	1.44	2.14	1.80	1.68	1.30	1.83
PaLM1-540B	1.88	0.54	1.33	2.01	1.58	1.57	1.25	1.68
PaLM2-XXS	2.37	0.87	1.77	2.46	2.17	1.96	1.38	1.96
PaLM2-XS	2.12	0.73	1.53	2.22	1.92	1.72	1.27	1.72
PaLM2-S	1.95	0.60	1.37	2.06	1.71	1.57	1.19	1.55
PaLM2-M	1.88	0.56	1.31	1.99	1.59	1.51	1.12	1.48
PaLM2-L	1.75	0.46	1.23	1.88	1.22	1.43	1.08	1.36

Table 5. Log-perplexity (NLL) scores evaluated on the first 2048 tokens, after trimming the first 100 tokens, of documents belonging to each of the shown domains. Only documents with a minimum length of 4K tokens are used.

Model	OpenWebText2	Github	FreeLaw	Pile-CC	Wikipedia	PubMed	Mathematics	ArXiv
T5-Decoder-110M	0.58 ± 0.04	0.67 ± 0.03	0.51 ± 0.02	0.54 ± 0.07	0.59 ± 0.04	0.59 ± 0.03	0.51 ± 0.04	0.58 ± 0.05
T5-Decoder-340M	0.52 ± 0.03	0.59 ± 0.05	0.63 ± 0.04	0.58 ± 0.04	0.61 ± 0.03	0.61 ± 0.03	0.48 ± 0.04	0.61 ± 0.05
T5-Decoder-1B	0.54 ± 0.01	0.66 ± 0.11	0.61 ± 0.06	0.57 ± 0.06	0.59 ± 0.05	0.60 ± 0.02	0.50 ± 0.03	0.63 ± 0.02
T5-Decoder-5B	0.51 ± 0.04	0.70 ± 0.04	0.60 ± 0.04	0.58 ± 0.02	0.58 ± 0.03	0.57 ± 0.02	0.45 ± 0.02	0.67 ± 0.05
PaLM1-8B	0.56 ± 0.03	0.67 ± 0.05	0.63 ± 0.05	0.58 ± 0.01	0.55 ± 0.04	0.62 ± 0.03	0.50 ± 0.03	0.68 ± 0.07
PaLM1-62B	0.49 ± 0.03	0.65 ± 0.09	0.63 ± 0.09	0.57 ± 0.03	0.63 ± 0.05	0.61 ± 0.04	0.48 ± 0.05	0.68 ± 0.03
PaLM1-540B	0.51 ± 0.04	0.68 ± 0.09	0.64 ± 0.05	0.58 ± 0.04	0.67 ± 0.03	0.64 ± 0.08	0.48 ± 0.03	0.65 ± 0.04
PaLM2-XXS	0.53 ± 0.02	0.61 ± 0.05	0.58 ± 0.04	0.60 ± 0.04	0.57 ± 0.05	0.61 ± 0.03	0.52 ± 0.02	0.70 ± 0.04
PaLM2-XS	0.54 ± 0.04	0.57 ± 0.06	0.58 ± 0.03	0.56 ± 0.04	0.60 ± 0.04	0.57 ± 0.06	0.45 ± 0.02	0.73 ± 0.06
PaLM2-S	0.55 ± 0.02	0.55 ± 0.15	0.59 ± 0.02	0.54 ± 0.08	0.65 ± 0.04	0.58 ± 0.05	0.49 ± 0.04	0.61 ± 0.03
PaLM2-M	0.58 ± 0.02	0.62 ± 0.06	0.59 ± 0.04	0.60 ± 0.05	0.70 ± 0.03	0.56 ± 0.04	0.46 ± 0.04	0.62 ± 0.05
PaLM2-L	0.53 ± 0.05	0.60 ± 0.05	0.61 ± 0.05	0.56 ± 0.03	0.62 ± 0.02	0.60 ± 0.07	0.42 ± 0.03	0.70 ± 0.03

Table 6. Self-similarity exponent S evaluated on the first 2048 tokens, after trimming the first 100 tokens, of documents belonging to each of the shown domains. Only documents with a minimum length of 4K tokens are used.

Fractal Patterns May Unravel the Intelligence in Next-Token Prediction

Model	OpenWebText2	Github	FreeLaw	Pile-CC	Wikipedia	PubMed	Mathematics	ArXiv
T5-Decoder-110M	0.63 ± 0.00	0.82 ± 0.01	0.62 ± 0.01	0.67 ± 0.01	0.62 ± 0.01	0.65 ± 0.00	0.54 ± 0.01	0.68 ± 0.01
T5-Decoder-340M	0.63 ± 0.01	0.82 ± 0.01	0.62 ± 0.00	0.67 ± 0.00	0.62 ± 0.01	0.64 ± 0.01	0.54 ± 0.00	0.67 ± 0.01
T5-Decoder-1B	0.63 ± 0.01	0.83 ± 0.01	0.63 ± 0.01	0.67 ± 0.00	0.62 ± 0.01	0.64 ± 0.00	0.54 ± 0.00	0.67 ± 0.00
T5-Decoder-5B	0.63 ± 0.01	0.82 ± 0.00	0.62 ± 0.01	0.67 ± 0.01	0.62 ± 0.01	0.64 ± 0.01	0.54 ± 0.00	0.67 ± 0.00
PaLM1-8B	0.65 ± 0.01	0.81 ± 0.01	0.66 ± 0.00	0.68 ± 0.01	0.66 ± 0.00	0.65 ± 0.01	0.57 ± 0.00	0.69 ± 0.01
PaLM1-62B	0.66 ± 0.01	0.80 ± 0.00	0.67 ± 0.01	0.69 ± 0.01	0.68 ± 0.00	0.65 ± 0.00	0.57 ± 0.00	0.70 ± 0.00
PaLM1-540B	0.67 ± 0.00	0.79 ± 0.01	0.68 ± 0.00	0.69 ± 0.01	0.71 ± 0.01	0.65 ± 0.01	0.56 ± 0.00	0.70 ± 0.01
PaLM2-XXS	0.65 ± 0.01	0.81 ± 0.01	0.65 ± 0.01	0.68 ± 0.01	0.66 ± 0.01	0.65 ± 0.01	0.58 ± 0.00	0.71 ± 0.01
PaLM2-XS	0.65 ± 0.01	0.81 ± 0.01	0.66 ± 0.01	0.68 ± 0.01	0.67 ± 0.00	0.65 ± 0.00	0.56 ± 0.01	0.71 ± 0.01
PaLM2-S	0.67 ± 0.01	0.80 ± 0.01	0.66 ± 0.01	0.69 ± 0.00	0.68 ± 0.01	0.65 ± 0.01	0.54 ± 0.00	0.71 ± 0.00
PaLM2-M	0.67 ± 0.01	0.80 ± 0.01	0.67 ± 0.01	0.70 ± 0.01	0.70 ± 0.01	0.65 ± 0.01	0.52 ± 0.01	0.72 ± 0.01
PaLM2-L	0.68 ± 0.01	0.79 ± 0.01	0.68 ± 0.00	0.70 ± 0.00	0.74 ± 0.01	0.65 ± 0.00	0.50 ± 0.01	0.72 ± 0.01

Table 7. Hurst exponent H evaluated on the first 2048 tokens, after trimming the first 100 tokens, of documents belonging to each of the shown domains. Only documents with a minimum length of 4K tokens are used.

Model	OpenWebText2	Github	FreeLaw	Pile-CC	Wikipedia	PubMed	Mathematics	ArXiv
T5-Decoder-110M	0.44 ± 0.01	0.53 ± 0.00	0.42 ± 0.00	0.49 ± 0.01	0.45 ± 0.00	0.43 ± 0.00	0.33 ± 0.00	0.45 ± 0.00
T5-Decoder-340M	0.44 ± 0.02	0.53 ± 0.00	0.43 ± 0.00	0.49 ± 0.00	0.45 ± 0.01	0.43 ± 0.00	0.33 ± 0.00	0.45 ± 0.00
T5-Decoder-1B	0.43 ± 0.01	0.53 ± 0.00	0.43 ± 0.01	0.49 ± 0.01	0.45 ± 0.01	0.42 ± 0.00	0.33 ± 0.00	0.45 ± 0.01
T5-Decoder-5B	0.43 ± 0.01	0.53 ± 0.00	0.44 ± 0.00	0.49 ± 0.01	0.45 ± 0.00	0.42 ± 0.00	0.34 ± 0.00	0.45 ± 0.00
PaLM1-8B	0.45 ± 0.00	0.51 ± 0.00	0.46 ± 0.00	0.49 ± 0.01	0.48 ± 0.01	0.44 ± 0.01	0.34 ± 0.00	0.48 ± 0.01
PaLM1-62B	0.45 ± 0.00	0.50 ± 0.01	0.47 ± 0.00	0.49 ± 0.01	0.49 ± 0.00	0.44 ± 0.00	0.33 ± 0.00	0.48 ± 0.01
PaLM1-540B	0.46 ± 0.01	0.49 ± 0.01	0.47 ± 0.00	0.50 ± 0.01	0.50 ± 0.00	0.44 ± 0.00	0.33 ± 0.01	0.48 ± 0.00
PaLM2-XXS	0.44 ± 0.01	0.50 ± 0.00	0.45 ± 0.00	0.50 ± 0.01	0.48 ± 0.00	0.45 ± 0.00	0.34 ± 0.00	0.49 ± 0.00
PaLM2-XS	0.45 ± 0.01	0.50 ± 0.01	0.46 ± 0.01	0.49 ± 0.00	0.48 ± 0.00	0.44 ± 0.00	0.33 ± 0.01	0.49 ± 0.00
PaLM2-S	0.45 ± 0.00	0.49 ± 0.00	0.47 ± 0.00	0.50 ± 0.01	0.50 ± 0.01	0.44 ± 0.00	0.31 ± 0.00	0.49 ± 0.00
PaLM2-M	0.45 ± 0.01	0.49 ± 0.01	0.48 ± 0.01	0.50 ± 0.01	0.50 ± 0.00	0.44 ± 0.00	0.29 ± 0.00	0.49 ± 0.01
PaLM2-L	0.46 ± 0.01	0.49 ± 0.00	0.49 ± 0.00	0.50 ± 0.00	0.52 ± 0.00	0.44 ± 0.00	0.28 ± 0.00	0.49 ± 0.00

Table 8. Joseph exponent J evaluated on the first 2048 tokens, after trimming the first 100 tokens, of documents belonging to each of the shown domains. Only documents with a minimum length of 4K tokens are used.

C. Predicting Downstream Performance

Table 9 presents detailed downstream performance results, along with corresponding upstream metrics.

In Table 10, we repeat the same analysis in Section 3 using the adjusted R^2 coefficient, but with the self-similarity S and Joseph exponents J. Unlike in the median Hurst exponent, we do not observe any improvement when combining perplexity scores with the self-similarity exponent S or the Joseph exponent J.

Fractal Patterns May Unravel the Intelligence in Next-Token Prediction

Model	BPB	0S BBH Direct	0S BBH CoT	0S MMLU	3S BBH Direct	3S BBH CoT	5S MMLU	8S GSM8K CoT	0S BBH +MMLU	FS BBH +MMLU +GSM8K
T5-Decoder-110M	1.11	0.83	0.11	25.65	21.36	5.69	25.62	0.91	13.06	13.35
T5-Decoder-340M	1.00	0.96	0.17	25.72	23.57	10.03	25.98	1.59	13.14	14.79
T5-Decoder-1B	0.92	1.29	0.14	25.99	24.26	13.19	24.82	1.14	13.35	14.90
T5-Decoder-5B	0.85	2.13	0.48	24.41	24.76	18.05	25.63	2.20	12.86	16.41
PaLM1-8B	0.78	6.46	1.21	23.53	32.18	27.60	24.56	5.16	13.68	19.87
PaLM1-62B	0.70	13.79	0.83	51.86	39.51	39.70	54.78	29.57	29.59	41.32
PaLM1-540B	0.66	23.26	4.72	67.78	52.44	56.02	70.50	56.79	40.89	60.51
PaLM2-XXS	0.81	8.99	0.13	25.26	30.71	26.08	24.72	2.96	14.91	18.69
PaLM2-XS	0.73	16.68	0.95	49.69	38.28	37.64	47.42	22.14	29.25	35.84
PaLM2-S	0.67	23.60	4.24	69.89	48.88	50.88	68.12	50.49	41.91	56.16
PaLM2-M	0.65	21.32	5.70	69.62	52.49	56.04	69.33	59.21	41.57	60.94
PaLM2-L	0.61	24.00	10.19	79.10	66.34	66.66	78.64	80.36	48.10	75.17

Table 9. Full downstream few-shot evaluation results compared to upstream BPB. Here, BPB is computed over The Pile validation split using the first 2048 tokens of every document. All evaluation results are reported as raw (un-normalized) accuracy.

Please note that our results are not directly comparable to all previous published results for the same models; please cite the original results from (Chowdhery et al., 2022; Anil et al., 2023b). Here, we only aim for a fair comparison between models: only pretrained models without instruction tuning are used, we do not optimize any prompts for each model, and we evaluate all models using only a 2K sequence length.

	BPB	S	J	BPB+S	BPB+J
0S BBH Direct	0.785	-0.060	0.673	0.761	0.794
0S MMLU	0.653	-0.067	0.426	0.614	0.614
0S BBH+MMLU	0.685	-0.065	0.472	0.650	0.651
3S BBH Direct	0.767	-0.030	0.599	0.744	0.754
3S BBH CoT	0.881	-0.026	0.678	0.870	0.879
5S MMLU	0.660	-0.044	0.421	0.624	0.622
8S GSM8K CoT	0.654	-0.037	0.427	0.619	0.616
FS BBH + MMLU+GSM8K	0.717	-0.036	0.489	0.687	0.686

Table 10. Adjusted R^2 , which measures the proportion of variation in downstream performance (row) that is predictable from the given input(s) (column) using a trained linear regressor. Unlike in the median Hurst exponent, we do not observe any improvement when combining BPB scores with the self-similarity exponent S or the Joseph exponent J.